Available online at www.sciencedirect.com
ScienceDirect
Proceedings of the Combustion Institute 31 (2007) 2741–2748
Proceedings of the Combustion Institute
www.elsevier.com/locate/proci

Inhibition of atmospheric lean and rich $CH_4/O_2/Ar$ flames by phosphorus-containing compound

O.P. Korobeinichev [a,b,*], V.M. Shvartsberg [a], A.G. Shmakov [a], D.A. Knyazkov [a], I.V. Rybitskaya [b]

[a] *Institute of Chemical Kinetics and Combustion, Novosibirsk 630090, Russia*
[b] *Novosibirsk State University, Novosibirsk 630090, Russia*

Abstract

The mechanism of flame inhibition by phosphorus-containing species (PCSs) is known to involve their effect on the recombination of atoms and free radicals in flames. Chemical inhibition of laminar atmospheric methane/oxygen flames by trimethylphosphate over a range of equivalence ratio has been studied experimentally, using the heat flux method for measurement of burning velocity and molecular beam mass spectrometry for measurement of concentration profiles of both stable and labile species, and with numerical modeling using detailed chemical kinetic reaction mechanisms. Concentrations of H and OH in flames with and without the inhibitor were obtained by measurements and modeling. The addition of the inhibitor reduces the maximum concentrations of H and OH (in the reaction zone) in the lean and rich flame. This reduction is much larger in the rich flame than in the lean one. The concentration profiles of PCSs—PO, PO_2, HOPO, $HOPO_2$, and H_3PO_4 were measured and simulated for rich and lean flames stabilized on a flat burner. According to flame speed measurements for inhibited CH_4/air flames over a range of ϕ, the inhibition effectiveness E_i increases in the range of $\phi = 0.8$–1.2 and then decreases with a further increase of ϕ. The increase in E_i in the range $\phi = 0.7$–1.2 is attributed to a change of PCSs composition. The reduction in E_i for $\phi > 1.2$ can be explained by a decrease in the concentration of active PCSs due to an increase in the concentration of inactive species, such as CH_3PO_2 and other products of incomplete combustion of TMP. The inhibition effectiveness E_i versus ϕ correlates with change of H and OH concentration at addition of TMP in flame. Validation of the previously developed model for inhibition by PCSs has shown that in spite of some discrepancies it adequately describes many experimental results.

Keywords: Phosphorus; Inhibition; Flame structure; Burning velocity; Premixed flames

1. Introduction

Over the last 10–15 years, it has been shown by a number of investigators that the mechanism of flame inhibition by phosphorus-containing species (PCSs) involves their effect on the recombination of atoms and free radicals in flames [1–15]. This

* Corresponding author. Fax: +7 383 3307350.
E-mail address: korobein@kinetics.nsc.ru (O.P. Korobeinichev).

1540-7489/$ - see front matter © 2006 The Combustion Institute. Published by Elsevier Inc. All rights reserved.
doi:10.1016/j.proci.2006.07.120

reaction is catalyzed by phosphorus oxides and phosphorus acids. As fire suppressants phosphorus-containing compounds have a number of distinctive features. One fundamental concept that seems to be especially important is that phosphorus can exist in more than one valence state, thereby giving it more ways to remove radical species from a flame and inhibit oxidation.

The foundation for research on the mechanism of flame inhibition by PCSs was laid by Hastie [1] and Twarowski [2–4]. The mechanism of flame inhibition by phosphorus compounds has been significantly supplemented and modified by the joint efforts of the group of Westbrook and the authors of the present paper [11,12].

Advances in the understanding of the inhibition mechanism and the development of the kinetic model have been made possible by systematic studies of the structures of the flame of various compositions containing PCSs. Previously, using molecular beam mass spectrometry (MBMS), we studied the structure of $H_2/O_2/Ar$ and $CH_4/O_2/Ar$ flames doped with trimethylphosphate (TMP) at low pressures [10] and the structure of $C_3H_8/O_2/Ar$ flames at atmospheric pressure over a range of equivalence ratio [11]. In particular, we measured the concentration profiles of active H, O, OH, and PCSs species in a low-pressure $H_2/O_2/Ar$ flame. Nogueira et al. [16] studied the structure of rich and stoichiometric methane–oxygen flames doped with dimethyl methylphosphonate (DMMP) at a near-atmospheric pressure by microprobe sampling with subsequent FTIR spectroscopic analysis of the products. Authors measured the concentrations of intermediate stable species—CH_2O, CH_3OH, and all C_2 hydrocarbons in the flame. In addition, they simulated the structure of the flames using the early models [9] and [8]. The results show that none of the models [8,9] provides an adequate description of the concentration profiles of the compounds tested. The structure and velocity of atmospheric premixed propane–oxygen flames with the addition of TMP was studied in [11,12]. It was shown that a change in the stoichiometric composition of the combustible mixture leads to a change in the composition of the PCSs, thus changing the inhibition effectiveness. However, the concentration profiles of atoms and radical were not measured in that work. Their changes in the presence of inhibitors provide valuable information on the role of each of the radicals in the inhibition chemistry. Calculations predicted that the inhibition effectiveness increases with increasing equivalence ratio. However, flame velocity measurements using a Mache–Hebra nozzle burner [17] and the total area method from an image of the flame [18] did not provide strong evidence in favor of or against this prediction because of insufficient accuracy.

The objective of this work is, to verify the previously developed mechanism of flame inhibition by PCSs by comparing various data on $CH_4/O_2/Ar$ flame structure and burning velocity at atmospheric pressure over a range of equivalence ratio. This problem is solved using various methods: (1) molecular beam mass spectrometry (MBMS) for concentration measurements of both stable and labile flame species (atoms and free radicals, phosphorus-containing species); (2) the microthermocouple technique for temperature profile measurements; (3) the heat flux method for measuring the burning velocity.

2. Experiments

Premixed laminar flames were stabilized on a Botha-Spalding flat burner 16 mm in diameter at atmospheric pressure and a slightly elevated temperature of unburned gases of about 380 K. Lean (0.06/0.15/0.79, $\phi = 0.8$) and rich (0.075/0.125/0.80, $\phi = 1.2$) combustible $CH_4/O_2/Ar$ mixtures were prepared using mass flow controllers (MKS Systems Inc., model 1299 S) with a total volumetric flow rate of 1.5 slm. TMP (2200 ppm) was added to the combustible mixtures using a saturator with liquid TMP in a controlled temperature bath.

The profiles of species concentrations were measured by MBMS with soft ionization by electron impact described previously [19]. The mass peaks corresponding to H, OH, and PCSs were measured at low ionization energy of electrons (IE) to avoid the contribution of fragmentary ions to the measured peaks. The IEs for each of the measured peaks are given in [20].

Systematic errors in measuring mass peak intensities depended strongly on the concentration of the corresponding species and the background peak intensity and were not higher than 5% (relative) for stable species, 10–15% for H and OH; for PCSs they were 15% for PO, PO_2, and HOPO, 20% for $HOPO_2$, and 25–30% for $(HO)_3PO$. The large measurement errors for peaks at 80 and 98 amu are due to the high intensities of the corresponding background peaks.

The calibration coefficients for H, O, and OH were determined based on partial equilibrium by three "rapid" reactions in the undoped lean flame: $H_2 + OH = H_2O + H$, $H_2 + O = H + OH$, and $O_2 + H = OH + O$ similarly to [20]. It should be noted that this method is standard for the calibration of mass spectrometers for radicals.

Temperature profiles in the flames were measured by Pt−Pt+10%Rh Π-shape thermocouples welded from wire 0.02 mm in diameter, covered by a thin layer of SiO_2 to prevent catalytic recombination of radicals on their surfaces. The resulting thermocouple junction has a diameter of 0.03 mm and a shoulder length of about 3 mm, providing negligible heat losses. The junction of the thermocouple was located at a distance of 0.25 mm from the tip of the probe. Further details

of the thermocouple design can be found elsewhere [21].

The burning velocity was measured using the heat flux method described in [22]. The setup design was similar to that in [22]. The burner consisted of a tube 15 cm high with an attached copper disk 24 mm in diameter and 3 mm thick with 0.5 mm diameter orifices spaced 0.7 mm apart. The burner temperature was kept constant at 368 K by means of a thermostat. The initial temperature of the combustible methane–air mixture was maintained at 308 K. The radial temperature distribution on the burner surface was measured by six copper-constantan thermocouples soldered into the burner orifice.

According to the data of [22], the systematic error of flame velocity measurements using this method is 3% and its maximum values are observed for substantially non-stoichiometric flames. However, in the experiments described here, the maximum error was 4%.

3. Modeling approach

The simulation of flame structure and burning velocity calculations were performed with the use of PREMIX and CHEMKIN codes. Experimentally measured temperature profiles were used as input data for flame structure simulations.

The flame structure was simulated using a mechanism for hydrocarbon oxidation up to C_3H_8 consisting of 469 reactions, which involve 77 species (H, O, C, and N) [23,24].

In the calculations of the burning velocity, the GRI 3.0 mechanism was also used for methane oxidation [25]. A comparison of the calculated and experimental results for the burning velocity of undoped flames shows that the speed of nearly stoichiometric flames is more accurately predicted by the GRI 3.0 mechanism than mechanism [23,24]. The speed of flames with $\phi = 0.8$ and 1.2 is predicted by both mechanisms with identical accuracy.

The mechanism of flame inhibition by PCSs was developed previously [11,12] and included 210 elementary stages and 41 species. This mechanism is available on the website [15].

4. Results and discussion

4.1. Influence of TMP on the temperature and concentration of radicals in lean and rich flames

Figure 1 shows temperature profiles in the lean and rich flames without and with the addition of 0.22% TMP. It is evident from Fig. 1 that the addition of the inhibitor leads to an increase in the width of the combustion zone and an increase in the final temperature of the flames due to a reduction of heat losses to the burner.

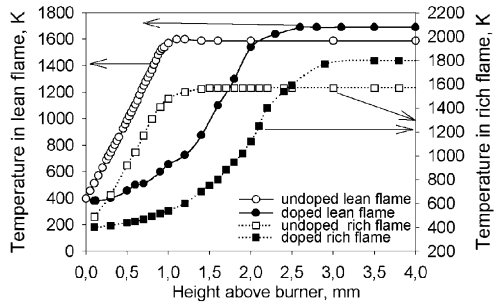

Fig. 1. Profiles of temperature in the lean (squares) and rich $\phi = 1.2$ (circles) flames without additives (open symbols) and doped with 2200 ppm of TMP (filled symbols).

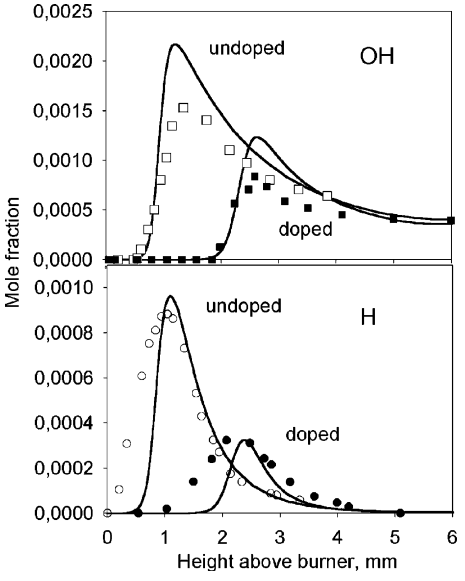

Fig. 2. Profiles of concentration of H and OH in the lean $\phi = 0.8$ $CH_4/O_2/Ar$ flame without additives and doped with 2200 ppm of TMP (symbols—experiment, lines—modeling).

Figure 2 gives measured and calculated concentration profiles of H and OH in the lean flame without and with the addition of TMP. One can see that the addition of the inhibitor leads to a factor of ≈3 decrease in the maximum H concentration and a factor of 2–2.5 decrease in the maximum OH concentration. At the same time, in the post-flame zone (at a distance of 4 mm from the burner surface), the concentrations of H and OH remain almost unchanged with the addition of the inhibitor. The simulation results are in satisfactory agreement with the experimental data for this flame.

In the rich flame, the H and OH concentration profiles (Fig. 3) change differently. First, one

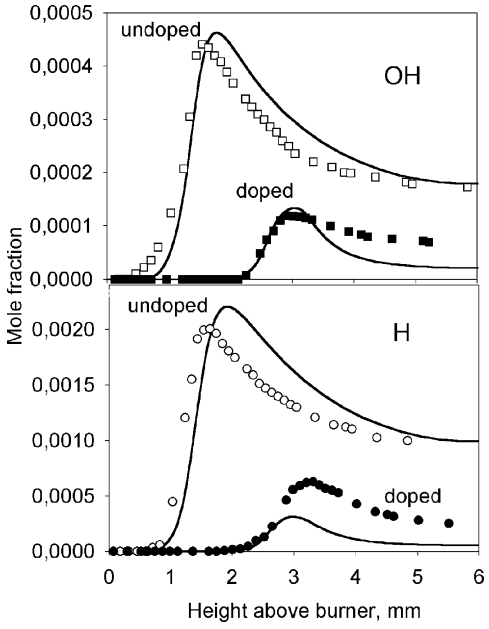

Fig. 3. Profiles of concentration of H and OH in the rich $\phi = 1.2$ $CH_4/O_2/Ar$ flame without additives and doped with 2200 ppm of TMP (symbols—experiment, lines—modeling).

observes a larger (a factor of 4–4.5) reduction in the maximum concentrations upon the addition of the inhibitor of the same concentration. Second, there is a several-fold difference in the final concentrations of the radicals between the flames without and with the additive. Consequently, in the rich flame, the inhibition effectiveness (the reduction in H and OH concentrations) is higher in both the post-flame and the reaction zone.

A comparison of the measured and simulated concentration profiles of H and OH in the rich flame shows that the kinetic model adequately describes the experimental data for undoped flame. The discrepancy for the doped flame may be attributed to imperfection of inhibition model and (or) to the low concentration of H and OH in this flame, resulting in a low accuracy in the measurement of the intensity of the corresponding peak.

The data suggest that the addition of TMP to both the lean and rich flames reduces the maximum concentrations of H and OH radicals (their concentrations in the reaction zone). A different situation is observed for the H and OH concentrations in the post-flame zone. In the lean flames with and without the additive, the H and OH concentrations in the flames coincide, whereas for the rich doped flame, the H and OH concentrations are 3–4 times lower than their concentrations in the undoped flame. One might suggest that the change in the H and OH concentrations due to the additive is related to an increase in the final temperature of the flame (by 100 K in the lean flame and by 200 K in the rich flame). However, calculations have shown that a 100 K decrease in the final temperature of a freely propagating atmospheric CH_4/air flame due to dilution with nitrogen leads to a 40% decrease in the maximum concentration of H and a 60% decrease in the maximum concentration of OH. If the final temperature of the TMP-doped flame stabilized on a flat burner is reduced to the temperature of the undoped flame, the maximum concentrations of H and OH will become much lower than the values obtained in our experiment. In addition, as it was shown by the calculations, the final temperature of an adiabatic CH_4/air lean ($\phi = 0.8$) and rich ($\phi = 1.2$) flame doped with 2200 ppm of TMP, changes only slightly, whereas the maximum concentrations of H and OH decrease by a factor of 3.6–3.8. Thus, the reduction in the H and OH concentrations in the flame due to the addition of inhibitor can be used as a measure of inhibitor effectiveness.

Table 1 gives the final concentrations of H and OH in the atmospheric lean and rich flames without and with TMP additives obtained by simulation and calculated using the conditions of partial (for three fast reactions) and complete thermodynamic equilibrium. Experimental and simulated concentrations of PCSs in the post-flame zone and the results of calculation of these concentrations on the basis of thermodynamic equilibrium are presented in Table 2. The data of Tables 1 and 2 show that in the atmospheric flames without additives, equilibrium for the radicals is not established, whereas in the TMP-doped flames, the concentration of H, OH, and PCSs are close to the equilibrium values.

In the undoped flames, the simulation and calculations using the conditions of partial equilibrium give almost similar values for the H and OH concentrations in the post-flame zone. In the lean TMP-doped flame, these concentrations differ by a factor of 1.5–2. In the TMP-doped rich flame, the simulated concentrations of H and OH differ considerably from those determined using the partial equilibrium conditions, especially for H atoms, whose concentration is two orders of magnitude lower than the concentration determined from the partial equilibrium conditions. On addition, from the data in Table 1 it follows that the relative decreases in the H and OH concentrations in the post-flame zone due to TMP additive is larger in the rich flame than in the lean flame.

All these distinctions indicate that in atmospheric-pressure TMP-doped flames, the rate of H and OH consumption in the reactions of the radicals with PCSs is markedly higher than the rate of their formation by fast reactions. The catalytic pathways involving reactions of H and OH with PCSs species provide additional, faster

Table 1
Simulated, equilibrium (EQ) and determined from conditions of partial equilibrium (partial EQ) concentrations of H and OH in post-flame zone (at 5 mm above burner) in lean and rich $CH_4/O_2/Ar$ flames without additive and doped with TMP

Species	$CH_4/O_2/Ar$ flames doped with 0.22% (by volume) of TMP					
	Rich flame, $T_f = 1800$ K			Lean flame, $T_f = 1690$ K		
	EQ	Modeling	Partial EQ	EQ	Modeling	Partial EQ
H	6.00×10^{-5}	5.78×10^{-5}	2.3×10^{-3}	5.40×10^{-7}	3.88×10^{-6}	6.5×10^{-6}
OH	1.60×10^{-5}	2.13×10^{-5}	9.9×10^{-4}	2.00×10^{-4}	3.59×10^{-4}	5.8×10^{-4}
	$CH_4/O_2/Ar$ flames without additive					
	Rich flame, $T = 1570$ K			Lean flame, 1590 K		
	EQ	Modeling	Partial EQ	EQ	Modeling	Partial EQ
H	5.95×10^{-6}	1.00×10^{-3}	1.0×10^{-3}	9.77×10^{-8}	6.15×10^{-6}	6.9×10^{-6}
OH	1.07×10^{-6}	1.80×10^{-4}	1.9×10^{-4}	1.04×10^{-4}	4.09×10^{-4}	4.6×10^{-4}

Table 2
Mole fraction of phosphorus species related to mole fraction of phosphorus in the post-flame zone (at 5 mm above burner, experiment—exp, modeling—mod) and in equilibrium (equil) in the lean and rich $CH_4/O_2/Ar$ flames doped with 2200 of TMP

Flame	Species	Mole fraction		
		Exp	Mod	Equil
LEAN	PO	≈0	≈0	0
	PO_2	0.015	0.018	0.011
	HOPO	0.007	0.006	0.006
	$HOPO_2$	0.87	0.90	0.90
	H_3PO_4	0.08	0.068	0.068
RICH	PO	0.01	0.008	0.005
	PO_2	0.07	0.074	0.06
	HOPO	0.74	0.77	0.77
	$HOPO_2$	0.10	0.097	0.064
	H_3PO_4	0	0.003	0.002

kinetic routes and accelerate the approach of the system to chemical equilibrium. Possible reasons for the different rates of catalytic chain termination in the lean and rich flames have been studied earlier [11].

4.2. Postflame phosphorus-containing species

Figures 4 and 5 present measured and simulated concentration profiles of PCSs—PO, PO_2, HOPO, $HOPO_2$, and $(HO)_3PO$ in the lean and rich flames, respectively. The results obtained earlier demonstrate that an insignificant change in the composition of the combustible mixture leads to significant changes in the composition of the final PCSs. In the lean flame, $HOPO_2$ is the main phosphorous-containing product (about 90% of the total amount of phosphorus in the flame). In the rich flame, most of the phosphorus (75%) is contained in HOPO.

A comparison of the calculation results for the model of [11,12] and experimental data indicates that they are in good agreement with respect to the main components—$HOPO_2$ in the lean and HOPO in the rich flame. However, for other PCSs, the agreement is not so good.

The modeling shows that in addition to PO, PO_2, HOPO, $HOPO_2$, and $(HO)_3PO$, the final phosphorus-containing products in the rich flame contain about 5% (of the total amount of phosphorus) CH_3PO_2, which does not catalyze the recombination of radicals. It can be assumed that increasing of excess of fuel ($\phi > 1.2$) will lead to an increase in the final concentration of CH_3PO_2 (and, probably, other low-activity compounds), resulting in a decrease in the concentration of radical scavengers and a reduction in the inhibition effectiveness of PCSs in rich flames.

4.3. Inhibition of freely propagating flames over a range of equivalence ratio

The influence of DMMP additive on the speed of C_3H_8/air flames over the range of equivalence ratio $\varphi = 0.8$–1.3 has been studied experimentally and by modeling [12]. Modeling predicted that the

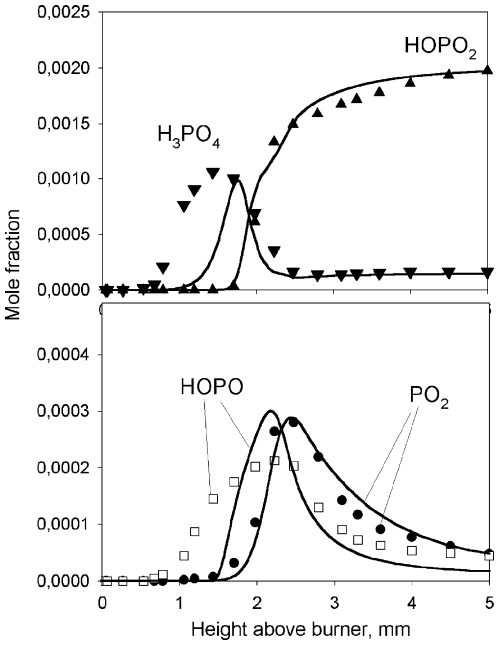

Fig. 4. Profiles of concentration of phosphorus-containing species in the lean $\phi = 0.8$ $CH_4/O_2/Ar$ flame doped with 2200 ppm of TMP (symbols—experiment, lines—modeling).

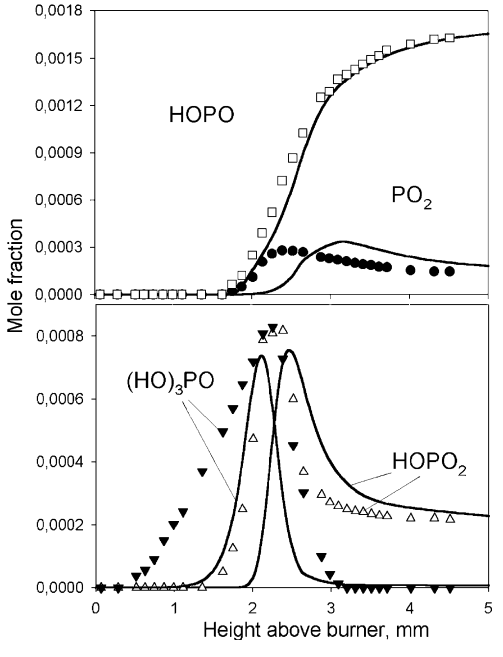

Fig. 5. Profiles of concentration of phosphorus-containing species in the rich $\phi = 1.2$ $CH_4/O_2/Ar$ flame doped with 2200 ppm of TMP (symbols—experiment, lines—modeling).

inhibition effectiveness increases along with increase of ϕ. The experimental measurements using a Mache–Hebra nozzle burner [17] and the total area method [18] did not reveal such dependence.

In the present work, we carried out a similar study for CH_4/air flames over a range of equivalence ratio using one of the most accurate technique for flame speed measurements [22] in order to verify the dependence obtained earlier. According to [26] the error of flame speed measurement by the heat flux method provides the best accuracy of ±1% (at burning velocity 40 cm/s). But the application of counterflow flame, closed vessel or Mache–Hebra nozzle burner techniques gives the errors of 2.5% and 5%, respectively. Results of measurements and calculations of flame speed using two mechanisms for

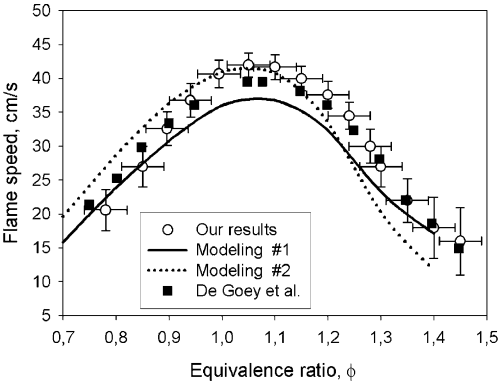

Fig. 6. Burning velocity in CH_4/air mixtures versus equivalence ratio; symbols—experiments (circles—our data, squares—data from Ref. [26]), lines—modeling (modeling #1 involves mechanism [23,24], modeling #2 involves mechanism [25]).

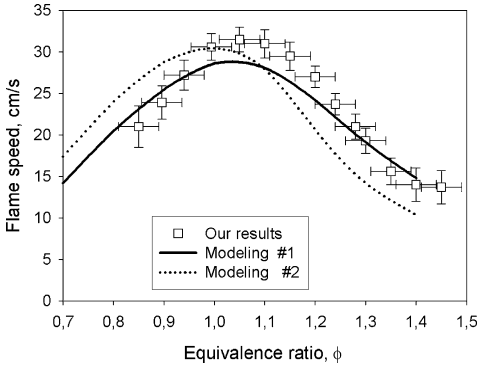

Fig. 7. Burning velocity of CH_4/air mixtures doped with 600 ppm of TMP versus equivalence ratio; symbols—experiments, lines—modeling (both modeling data were obtained using model for inhibition [11,12], #1 involves mechanism [23,24], #2 involves mechanism [25]).

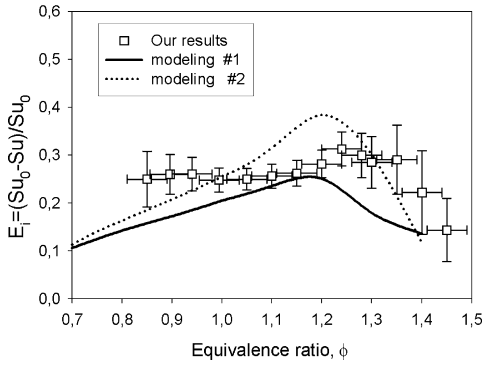

Fig. 8. Inhibition effectiveness versus equivalence ratio, symbols—experiments, lines—modeling (modeling #1 involves mechanism [23,24], modeling #2 involves mechanism [25]).

undoped flame and doped with 600 ppm of TMP are shown in Figs. 6 and 7. These mechanisms include the same set of reactions with PCSs [11,12] but different sets of reactions for methane oxidation—GRI 3.0 [25] and [23,24]. A comparison of the calculated and experimental results for the burning velocity of undoped flames shows that the speed of nearly stoichiometric flames is more accurately predicted by the GRI 3.0 mechanism. The speed of flames with $\phi = 0.8$–1.2 is predicted by both mechanisms with identical accuracy. In addition, Fig. 6 gives data [26] obtained using the same heat flux method, which agree well with our measurements. The predictions obtained using GRI 3.0 mechanism are in better agreement with experimental data for near-stoichiometric flames, whereas the mechanism of [23,24] provides the best fit for lean and rich flames. The observed discrepancies between the model predictions and measurements are likely due to the imperfection of the methane combustion model. The inhibition effectiveness E_i versus ϕ estimated from the experimental and modeling data is shown in Fig. 8. Modeling using both mechanisms predicts that E_i increases monotonically (by a factor of $\approx 2.5 \div 3.8$) as ϕ grows from 0.7 to 1.2, after which it decreases to 1.8 at $\phi = 1.4$. The experimental dependence of E_i versus ϕ differs from the calculated results. A similar dependence was obtained for DMMP-doped C_3H_8/Air flames [12].

It is noteworthy that for freely propagating H_2/O_2/Ar flames without and with a small addition of TMP (<0.12%) at 1 atm, flame speed calculations using the inhibition mechanism [11,12] do not predict a noticeable change in the inhibition effectiveness over a range of $\phi = 0.8$–1.4. The decrease E_i for $\phi > 1.2$ can be attributed to a drop of the concentration of active PCSs as the concentration of CH_3PO_2 increases from 0 to 5% of the total amount of phosphorus in the flame.

5. Conclusions

1. The addition of TMP to lean and rich CH_4/O_2/Ar flames decreases the maximum H and OH concentrations. This decrease is larger in the rich flame than in the lean one. But H and OH concentrations in post-flame zone do not change at addition of TMP in lean flame, whereas they decrease at addition of inhibitor to rich flame.
2. It is found that $HOPO_2$ is the main PCS in lean flames and HOPO in rich flames. In the post-flame zone of the inhibited flames, the concentrations of H, OH, PO, PO_2, HOPO, $HOPO_2$, and H_3PO_4 are close to the thermodynamic equilibrium values.
3. Calculations of speed of CH_4/air flames of various compositions in the range of $\phi = 0.7$–1.5 show that the inhibition effectiveness (expressed as the relative change in the flame speed) increases in the range $\phi = 0.7$–1.2 and decreases for $\phi > 1.2$. Experimental study does not reveal a growth of the inhibition effectiveness in the range of $\phi = 0.7$–1.2. The increase in the inhibition effectiveness in the range $\phi = 0.7$–1.2 predicted by modeling can be explained by an increase in the concentration of active PCSs, which catalyze the recombination of H and OH more effectively. The reduction of inhibition effectiveness for $\phi > 1.2$ probably is due to an increase in the concentration of inactive species such as CH_3PO_2 and other products of incomplete combustion of TMP in rich flames, which substitute active PCSs.
4. A comparison of the experimental and modeling results shows that the mechanism generally gives adequate predictions of flame speed and concentration profiles of stable and the majority of labile species in the flames. There are, however, some discrepancies between measured and simulated flame speeds as well as between measured and simulated concentration profiles of H and OH in the rich doped flame and concentration profiles of some PCSs, indi- cating that the kinetic model needs further refinement.

Acknowledgment

This work was supported by INTAS under Grant 03-51-4724.

References

[1] J.W. Hastie, D.W. Bonnell, Molecular Chemistry of Inhibited Combustion Systems, National Bureau of Standards, *NBSIR* 80-2169 (1980).

[2] A.J. Twarowski, *Combust. Flame* 94 (1993) 91–107.
[3] A.J. Twarowski, *Combust. Flame* 94 (1993) 341–348.
[4] A.J. Twarowski, *Combust. Flame* 102 (1995) 41–54.
[5] J.H. Werner, T.A. Cool, *Combust. Flame* 117 (1999) 78–98.
[6] O.P. Korobeinichev, S.B. Ilyin, V.V. Mokrushin, A.G. Shmakov, *Combust. Sci. Technol.* 116 (1996) 51–61.
[7] O.P. Korobeinichev, V.M. Shvartsberg, A.A. Chernov, V.V. Mokrushin, *Proc. Combust. Inst.* 26 (1996) 1035–1042.
[8] R.T. Wainner, K.L. McNesby, A.W. Daniel, A.W. Miziolek, and V.I. Babushok, in: *Halon Options Technical Working Conference (HOTWC)*, Albuquerque, NM, (2000) pp. 141–153.
[9] P.A. Glaude, C. Melius, W.J. Pitz, C.K. Westbrook, *Proc. Combust. Inst.* 29 (2002) 2469–2476.
[10] O.P. Korobeinichev, T.A. Bolshova, V.M. Shvartsberg, A.A. Chernov, *Combust. Flame* 125 (2001) 744–751.
[11] O.P. Korobeinichev, V.M. Shvartsberg, A.G. Shmakov, T.A. Bolshova, T.M. Jayaweera, C.F. Melius, et al., *Proc. Combust. Institute* 30 (2) (2005) 2350–2357.
[12] T.M. Jayaweera, C.F. Melius, W.J. Pitz, C.K. Westbrook, O.P. Korobeinichev, V.M. Shvartsberg, et al., *Combust. Flame* 140 (1–2) (2005) 103–115.
[13] T.M. Jayaweera, W.J. Pitz, C.K. Westbrook, in: Proceedings of the Third Joint Meeting of the U.S. Sections of The Combustion Institute, C39.
[14] J.C. Mackie, G.B. Bacskay, N.L. Haworth, *J. Phys. Chem. A* 106 (2002) 10825–10830.
[15] Available at http://www-cms.llnl.gov/combustion/combustion2.html#Organophos_Lean_and_Rich_Propane_Flm_2004.
[16] M.F.M. Nogueira, *E.M. Fisher. Combust. Flame* 132 (3) (2003) 352–363.
[17] H. Mache, A. Hebra, *Sitzungsber. Osterreich. Akad. Wiss., Abt. IIa* 150 (1941) 157.
[18] G.T. Linteris, G.T. Truett, *Combust. Flame* 105 (1996) 15–27.
[19] O.P. Korobeinichev, S.B. Ilyin, V.M. Shvartsberg, A.A. Chernov, *Combust. Flame* 118 (1999) 718–726.
[20] O.P. Korobeinichev, V.M. Shvartsberg, A.A. Chernov, *Combust. Flame* 118 (1999) 727–732.
[21] O.P. Korobeinichev, S.B. Ilyin, V.V. Mokrushin, A.G. Shmakov, *Combust. Sci. Technol.* 116 (1996) 51–61.
[22] I.V. Dyakov, A.A. Konnov, J. de Ruyck, K.J. Bosschaart, E.C.M. Brock, L.P.H. de Goey, *Combust. Sci. Technol.* 172 (2001) 81–96.
[23] H.J. Curran, in: Proceedings of the European Combustion Meeting, 2003.
[24] H.J. Curran, T.M. Jayaweera, W.J. Pitz, C.K. Westbrook, in: Western States Section of the Combustion Institute, Davis, California (2004) Paper No. 04S-58.
[25] G.P. Smith, D.M. Golden, M. Frenklach, N.W. Moriarty, B. Eiteneer, M. Goldenberg, C.T. Bowman, R.K. Hanson, S. Song, W.C. Gardiner Jr., V.V. Lissianski, and Z. Qin, GRI Mech 3.0, 1999, available at http://www.me.berkeley.edu/gri_mech/.
[26] K.J. Bosschaart, L.P.H. de Goey, *Combust. Flame* 136 (3) (2004) 261–269.